RGNZ/MGPB

Investigation of corrosion resistance of epoxy coatings reinforced with graphene oxide and aluminium nanoparticle

Rudarsko-geološko-naftni zbornik
(The Mining-Geology-Petroleum Engineering Bulletin)
DOI: 10.17794/rgn.2025.4.6

Original scientific paper

Marin Kurtela[1], Marina Samardžija[2]*, Maro Bujak[3], Ivan Stojanović[1], Krunoslav Bojanić[3], Gabrijela Ljubek[2]

[1] *University of Zagreb Faculty of Mechanical Engineering and Naval Architecture, Street Ivan Lučić 5, HR-10000 Zagreb, Croatia.*

[2] *University of Zagreb Faculty of Mining, Geology and Petroleum Engineering, Perottijeva 6, HR-10000 Zagreb, Croatia.*

[3] *Institute Ruđer Bošković, Bijenička c. 54, HR-10000 Zagreb, Croatia.*

Abstract

Graphene oxide (GO) is a two-dimensional carbon nanomaterial known for its exceptional mechanical strength and tunable, functional surface, making it a promising material for protective barriers against harmful external influences. For this purpose, it is used as a filler in epoxy coatings to increase the tortuous diffusion path of the corrosive medium within the coating. Additionally, the incorporation of aluminum nanoparticles (Al NP) onto the GO surface can improve the dispersion of GO sheets, reduce their aggregation, and maintain the passive oxidation film formed by the degradation of Al NP. In this study, epoxy coatings containing Al NP–GO powder with different weight fractions of GO material were prepared. The physical, anticorrosive, and antibacterial properties of unmodified and modified coatings were evaluated. On the macroscopic electrochemical micro-level, the EP+MAX sample provided stable corrosion protection for 60 days, whereas the resistance of other samples decreased. Measurements performed on micro-surfaces (500 μm) showed an increase in impedance per unit area with the addition of Al NPs-GO powder. The best corrosion resistance was demonstrated by the EP+MIN and EP+MAX samples. Furthermore, using the ic-dc microscopic SECM method, it was determined that Fe^{2+} dissolution at the scratch area was reduced in the modified samples. Additionally, it was found that the epoxy coating acquires new antibacterial properties, thus gaining dual functionality.

Keywords:
aluminium nanoparticles, antibacterial activity, corrosion protection, epoxy coating, graphene oxide

1. Introduction

Corrosion poses a significant challenge across various sectors, including the oil and gas industry, marine infrastructure, transportation systems, aircrafts, and irrigation networks, leading to both economic and society problems (**Aghili et al., 2021; Kumar et al., 2021**). Coating remains the predominant strategy for corrosion prevention, reduction, and control, largely due to the wide availability of diverse coating materials and application processes tailored to different operational conditions (**Kumar et al., 2021**). Although advancements in coating technologies have been substantial, long-term protection of metals from harsh environments continues to encounter challenges (**Abdeen et al., 2019**). Polymer nanocomposites use different approaches and aspects of nanotechnology and nanoscience to design and manufacture different types of surface coatings with outstanding properties that significantly improve the mechanical, tribological, antimicrobial and anticorrosive properties of metal substrates (**Kabeb et al., 2018**). The development of polymer nanocomposites has significantly expanded the possibilities of their application in corrosion protection thanks to their excellent properties. These materials enable increased hardness and improved adhesion of the coating, which provides longer lasting and more effective protection against corrosion. In addition, polymer nanocomposites improve the tribological properties of the surface. Due to all these advantages, polymer nanocomposites are increasingly used as anti-corrosion protection in various industries and are especially important in aviation, shipbuilding, and automotive (**Kim et al., 2010; Abu-Thabit et al., 2015; Chee at al., 2015; Abdeen et al., 2019; Moghaddam et al., 2019**). For the purpose of anti-corrosion protection, the epoxy coating stood out as one of the most effective types of polymer matrices. Epoxy coatings provide an outstanding surface barrier between the metal substrate and aggressive outdoor conditions, primarily due to their high resistance to moisture penetration, high fracture tough-

* Corresponding author: Marina Samardžija
e-mail address: marina.samardzija@rgn.unizg.hr
Received: 3 February 2025. Accepted: 24 February 2025.
Available online: 27 August 2025

ness and excellent bond strength (**Sadasivuni et al., 2015; Nguyen-tri et al. 2018; Muresan, 2023**). During long-term exposure of the epoxy coating to corrosive agents, its protective properties gradually weaken, which requires certain modifications to ensure long-term effectiveness (**Wu et al., 2019**). In view of these challenges, innovative nanocomposite coatings have been developed for the past ten years, enabling improved corrosion resistance properties. A key characteristic of nanocomposite coatings is their inclusion of at least two immiscible phases, with at least one component on the nanoscale. The main component in these coatings can be a metal nano particle that is evenly dispersed within the binder, thus producing a final product with improved properties.

This offers a significantly superior protective effect compared to the isolated performance of each constituent material (**Chee et al., 2015**). Nanoparticles, due to their extremely small dimensions (less than 100 nm), reinforce the matrix by filling the space inside the matrix, which prevents the diffusion of aggressive corrosive agents and thereby provides enhanced corrosion protection. Additionally, the strong interactions between the nano-filler and the matrix, significantly reduce porosity and cracking of the nanocomposite coating, minimizing issues such as blistering and delamination (**Kim et al., 2010**).

In recent years, driven by diverse industrial demands and practical applications, advanced protective coating technologies incorporating nanocomposites and carbon-based materials have garnered significant scientific interest. These technologies present a promising solution to mitigate harmful corrosion processes on material surfaces. Since its discovery and isolation in 2004, by the group of Andre Geim and Kontantin Novoselov, graphene has rapidly gained recognition as one of the most promising materials of the century. Graphene is an allotrope of carbon, consisting of one-atom-thick planar sheets of sp2-bonded carbon atoms densely packed in a honeycomb crystal lattice (**Ljubek et al., 2021**). Graphene and its derivatives have garnered significant attention as promising additives in anticorrosive coatings due to their remarkable properties, including excellent hydrophobicity, chemical resistance, thermal stability, and high mechanical strength. Their large surface area enhances their effectiveness as barrier materials, making them ideal candidates for applications in corrosion protection. Graphene oxide (GO), in particular, has demonstrated high water dispersibility owing to its hydrophilic nature, which results from the presence of oxygen-containing functional groups. These functional groups not only improve the dispersibility of GO but also facilitate chemical functionalization, thereby enhancing its corrosion inhibition performance (**Duan, 2019; Chauhan et al., 2020**).

Most organic coatings fall short in providing long-term corrosion protection, as corrosive agents like oxygen, aggressive electrolytes, and halogen elements can penetrate through material pores and reach the coating/metal interface during use. Therefore, leveraging graphene oxide (GO) nanoparticles is essential. GO in synergistic action with aluminum nanoparticles (Al NPs), significantly enhance the protective function of the coating, thereby preserving the integrity of the material's surface (**Mohammasi et al., 2014; Deyab et al., 2016**). The separate action of GO powder and Al NPs nanoparticles within the epoxy coating showed an outstanding ability to form a physical barrier that prevents the penetration of corrosive electrolytes through the coating. When the electrolyte penetrates the epoxy coating, it encounters the evenly distributed GO powder, which extends the diffusion path of corrosive molecules within the matrix, creating a labyrinth effect. This labyrinthine path makes it difficult for the electrolyte to move and thereby further reduces the rate of penetration of corrosive substances to the substrate. In addition to the physical effect, the presence of GO powder and Al NPs also provides an important chemical protection mechanism. These particles react with the electrolyte, creating a passive protective layer on the surface, as well as an antimicrobial film (**Quian et al., 2013; Karthikaiselvi et al., 2014**).

The aim of this work is to investigate the synergistic effect of aluminium nanoparticles in combination with graphene oxide to enhance and prolong the anticorrosive protection of metal structures. Aluminium nanoparticles have already proven to be a promising innovative solution in combating microbiologically induced corrosion, which poses a serious challenge to maintaining the durability and functionality of metal surfaces. On the other hand, graphene oxide provides exceptional barrier properties that extend the path of corrosive media through the epoxy matrix to the metal. By combining these two materials, it is expected that more effective protection will be achieved, potentially reducing the rate of metal degradation in aggressive conditions. The use of such advanced materials could open new possibilities for developing more effective and long-lasting coatings for metal protection.

To achieve the stated goals, this study examined the impact of aluminium nanoparticles in combination with various proportions of graphene oxide, which were incorporated into the epoxy coating. The objective was to investigate how this combination of materials affects the physical and anticorrosive properties of the coating, as well as its antibacterial properties. In order to analyze changes in physical properties, a series of tests were conducted, including measurements of hardness, adhesion, thickness, gloss, and colour of the epoxy coatings. Electrochemical testing at macro and micro levels was also carried out, which is crucial for determining how the addition of different proportions of graphene oxide and aluminum nanoparticles affects the resistance of the coatings in aggressive environments. The antibacterial

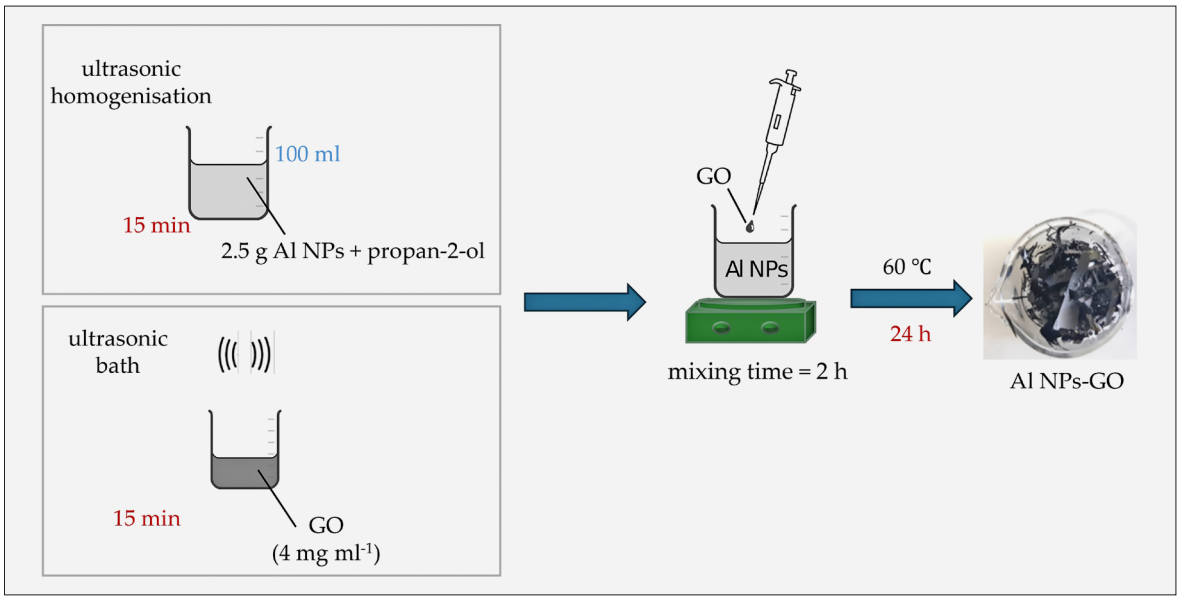

Figure 1. Graphical illustration of the preparation of Al NPs–GO powder

Table 1. Three formulations of prepared Al_NPs–GO powder

Samples	*m* (Al NPs), g	*V* (C_3H_8O), ml	*V* (GO), ml	*w* (GO), %
MIN	1.25	50	1.25	0.40
MID	1.25	50	3.20	1.00
MAX	1.25	50	6.20	2.00

Table 2. The composition of the prepared unmodified and modified epoxy coating with Al_NPs –GO powder

Samples	*m* (epoxy coating), g	*m* (hardener), g	*m* (Al_NPs–GO powder), g	Thickness, µm
EP	38	10	-	238.0
EP+MIN	38	10	0.4848	203.7
EP+MID	38	10	0.4848	214.3
EP+MAX	38	10	0.4848	227.5

properties of all prepared samples were further tested against two key bacterial strains: *Staphylococcus aureus* (*S. aureus*) and *Pseudomonas aeruginosa* (*P. aeruginosa*). These bacteria were chosen due to their significance, as they often contribute to the development of biofilms on metal surfaces, which can accelerate the corrosion process within pipelines.

2. Methods

2.1. Materials

- Graphene oxide water dispersion (0.4 wt.%) was purchased from Graphenea Inc., Cambridge, USA with >95% monolayer content and pH 2.2-2.5.
- The Al NPs materials, with an average particle size of approximately 100 nm, were supplied by Guangzhou Hongwu Material Technology Co., Ltd., China. The chemical composition of the nanoparticle powder consisted of 98.85% Al, 0.08% Cr, 0.03% Fe, and 1.04% residue (by weight).
- The prepared nanocomposites were applied to a base of grey cast iron (150×100×3 mm) whose chemical composition was 2.5 C, 1.5 Si, 1.05 Mn, 0.5 P, 0.07 S, and Fe in balance (wt.%). The dimensions of the samples.
- The epoxy coatings were prepared using diglycidyl ether of bisphenol A, with the polyamine hardener sourced from Hempel (Croatia).
- The bacterial strains used in investigation, Pseudomonas aeruginosa (PAO1) and Staphylococcus aureus (DSM 1104, SA) were purchased from DSMZ culture collection (Leibniz Institute, Germany).

2.2. Preparation of Al_NPs–GO epoxy nanocomposite

The first step in preparing Al_NPs-GO epoxy coating was to prepare a suspension of GO and Al NPs. **Figure 1** shows the powder preparation procedure of Al NPs

within GO. Initially, 2.5 g of Al NPs was added to 100 ml of propan-2-ol and mixed for 15 min using an ultrasonic homogenizer, with 5 cycles at an amplitude of 20%. The aqueous solution of GO was sonicated for 15 min. Subsequently, GO was gradually added to the prepared Al NPs to obtain Al_NPs-GO suspension. The suspension was stirred for 2 h, after which it was transferred to a Petri dish and dried at 60°C for 24 hours to obtain the Al_NPs-GO powder.

Three different Al_NPs-GO powders were prepared and named in the following order: minimum amount of GO (MIN), medium amount of GO (MID), and maximum amount of GO (MAX) (see **Table 1**).

The Al_NPs–GO epoxy coating was prepared by incorporating Al_NPs–GO powder into an epoxy matrix and mixed using an ultrasonic homogenizer for 10 minutes at 20% amplitude, with intermittent pauses to prevent overheating caused by the ultrasonic probe. The epoxy matrix was formulated by using epoxy paint and polyamine hardener in a mass ratio of 2:1. Four different coating formulations were prepared and shown in **Table 2**.

Before applying the coating, grey cast iron panels measuring 150 × 100 × 3 mm were abrasively blasted and cleaned with 70 wt.% ethanol. The prepared nanocomposite was then applied to the surface of the cast iron, using a film applicator (2×150 μm). The samples were analyzed after spending seven days at room temperature (25°C).

2.3. Analysis of the Al_NPs–GO epoxy coating

2.3.1. Physical properties

To investigate the influence of Al_NPs-GO powder on the physical properties of the epoxy coating, the hardness, adhesion, coating gloss, and colour tests were conducted. The samples' hardness was tested following ISO 868:2003. The coating hardness values were determined using the PosiTector SHD Shore Hardness Durometer (DeFelsko Corporation, USA).

The adhesion between the metal substrate and the polymer coatings was tested using an automatic Pull-Off Adhesion Tester (Elcometer 510, model T, UK). For this analysis, aluminium dollies (diameter 20 mm) were glued to the polymer coating using a two-component adhesive consisting of Araldite resin and Araldite hardener. After a period of 24 hours at room temperature (25°C), the samples were ready for adhesion measurement.

The gloss test was tested by TQC Gloss Meters (model GL0010 TQC SoloGloss 60°). The specular gloss of the samples was determined at 60° incident angle according to HRN EN ISO 2813 (**ISO 2813, 2000**).

The colour change due to the incorporation of Al-NPs--GO powder inside the epoxy coating was determined using the RAL colour chart (RAL gGmbH, Germany).

All measurements were performed after the samples were dried under atmospheric conditions for seven days.

2.3.2. Electrochemical impedance spectroscopy

Electrochemical impedance spectroscopy (EIS) measurements were conducted on the grey cast iron plates coated with unmodified and modified epoxy coating using a VersaSTAT 3 Instruments. The electrochemical cell consisted of three electrodes immersed in a 3.5 wt.% NaCl solution. The working electrode, featuring a test area of 19.75 cm², was made of grey cast iron plates coated with unmodified and modified epoxy coatings. A saturated calomel electrode (SCE) that was used as a reference electrode and a graphite electrode that served as an auxiliary electrode to close the circuit were the remaining two electrodes. The frequency scan range was from 100 kHz to 100 mHz, with a sinusoidal perturbation of 10 mV (RMS) × OCP. The ZSimpWin software (AMETEK, USA) (Version 3.2) was used to fit the impedance data.

2.3.3. Scanning electrochemical microscopy

A model Scanning electrochemical microscopy M470 was used to make measurements on unmodified and modified epoxy coatings. Two methods of measurement at the micro level were carried out.

Intermittent Contact-Scanning Electrochemical Microscopy (ic-ac-SECM) was used to observe the distribution of real impedance over a sample surface at 500 μm. During all experiments, the platinum tip was scanned at a constant height above the sample. These measurements were performed in a three-electrode electrochemical cell using tap water.

Cyclic voltametric measurements were performed by applying a potential of –0.7 mV to probe vs the Ag/AgCl/saturated KCl reference electrode. The electrochemical cell consisted of three electrodes immersed in a 3.5 wt.% NaCl solution. The scanning area of the UltraMicroElectrode (UME) was 2.5 mm in the x direction and 1 mm in the y direction. The scanning speed of the UME was 20 μm s^{-1} in the x direction.

For all measurements, a three-electrode system was employed, comprising an Ag/AgCl/KCl (saturated) reference electrode, a platinum sheet as the counter electrode, and a UME probe. The tip's movement was controlled in the x, y, and z directions using optically encoded inchworm piezo motors. A UME probe with a 10 μm diameter platinum wire was employed. During all experiments, the platinum tip was scanned at a constant height above the sample.

The vibration frequency of the UME was about 515 ± 5 Hz. The surface activity of the samples in 3D view was obtained using the 3DIsoPlot program.

2.3.4. Determination of biofilm inhibition

The biofilm inhibition was determined by the crystal violet (CV) method. The bacteria were cultured onto Tryptic Soy Agar (TSA, Biolife, Italy) overnight at

37°C. Each cell culture (10% microbial inoculum/medium, 0.5 MacFarland) was added to 6 wells plate containing Tryptic Soy Broth (TSB, Biolife, Italy), supplemented with 1% glucose with samples and incubated 24h at 37°C to determine the biofilm inhibition activity. After incubation, the broth with the planktonic cells was discarded by gently washing the wells three times with phosphate-buffered saline (PBS, Sigma-Aldrich) to remove unattached bacteria. Subsequently, the plate wells were dried for 2 hours at 65°C. The biofilms in the wells were stained using crystal violet (0.1 %, wt./vol) (Sigma-Aldrich, St. Louis, MO) for 30 minutes. Following staining, the wells were rinsed three times with PBS to remove any unbound dye. The crystal violet, which had adhered to the biofilms, was dissolved in 90% ethanol, and absorbance was measured at 590 nm using a microtiter plate reader (TECAN, Switzerland). All tests were performed in duplicate.

3. Results and discussion

3.1. Physical properties

Physical properties of the coating containing GO, enriched with Al NPs, were investigated. After the coatings have dried, the change in hardness, colour and adhesion of the coating to the metal substrate was tested depending on the addition of Al_NPs–GO powder inside the epoxy coating. The results for the physical properties of the epoxy coating, as well as the epoxy coatings with minimum, medium, and maximum amounts of Al_NPs–GO powder, are presented in **Table 3**.

The Pull-off adhesion test value indicates the impact of the sample preparation method on the adhesion of the protective coating to the metal surface of the samples (**Samardžija et al., 2022**). The obtained results clearly indicate that the addition of Al_NPs–GO powder, with varying amounts of GO into the epoxy coating, did not lead to significant changes in hardness and adhesion. This indicates that all formulations maintained good hardness and adhesion to the metal substrate. Furthermore, the angle of light measurement provides insight into the glossiness of the coatings. The pure epoxy coating had a gloss unit (GU) of 10.6, while the addition of Al_NPs–GO powder reduced the glossiness, with the minimum formulation at 5.1, the mid at 5.8, and the maximum at 8.0. This reduction in gloss indicates a transition from a glossy to a more matte finish. The decrease in gloss can be attributed to the rougher surface texture introduced by the nanoparticles, which tends to scatter light (**Samyn et al., 2015**).

However, by adding a larger amount of GO powder to the Al_NPs–GO, it can be observed that the EP+MAX sample had the smallest change in coating gloss, while the EP+MIN sample became the most matte, from which we can conclude that the coatings lose their gloss due to more free Al NPs that are not could be incorporated into the minimal added amount of GO powder. The colour assessment using the RAL colour chart shows a transition in colour with the addition of Al_NPs–GO. The pure epoxy coating is classified as RAL 9010 (Pure White), while the formulations with added nanoparticles shifted to RAL 7047, RAL 7045 and RAL 7046. This indicates a shift towards a grey hue with increasing Al_NPs–GO content.

Table 3. Results of physical properties for the unmodified epoxy coating, and modified epoxy coatings with Al_NPs–GO powder

Methods / Sample	Shore D hardness	Adhesion, (MPa)	Angle of light, (GU60°)	RAL
EP	85.6	7.0 7.1	10.6	9010
EP+MIN	84.6	7.5 8.1	5.1	7047
EP+MID	85.6	7.0 7.3	5.8	7045
EP+MAX	86.8	7.5 7.9	8.0	7046

3.2. Electrochemical measurement on macro level

Resistance to corrosive conditions of epoxy reference coating (EP) and modified epoxy coatings (MIN, MID, MAX) were tested by long-term exposure of 60 days in 3.5% NaCl solution, using the EIS technique. The impedance data were interpreted by numerical fitting in the equivalent circuit depicted in **Figure 2**, where R_e represents the electrolyte resistance, R_{coat} and CPE_{coat} denote the resistance and capacity of coating, CPE_{dl} representing the double layer capacitance between the coating/metal surface, and R_{ct} represent the charge transfer resistance across the metal surface (**Samardžija et al., 2024**).

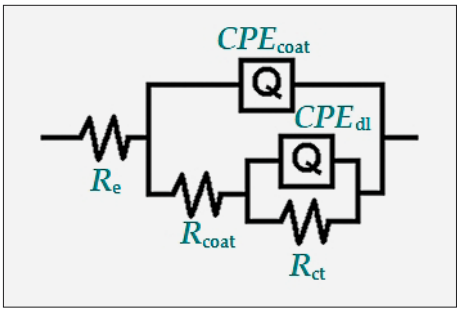

Figure 2. Equivalent circuit model used for fitting the impedance data of the unmodified and modified samples

The impedance plot obtained for grey cast iron, coated with epoxy, minimum, medium, and maximum amount of GO in Al NPs powder, for 14 days and 60 days of immersion in 3.5 wt.% NaCl solution, are dis-

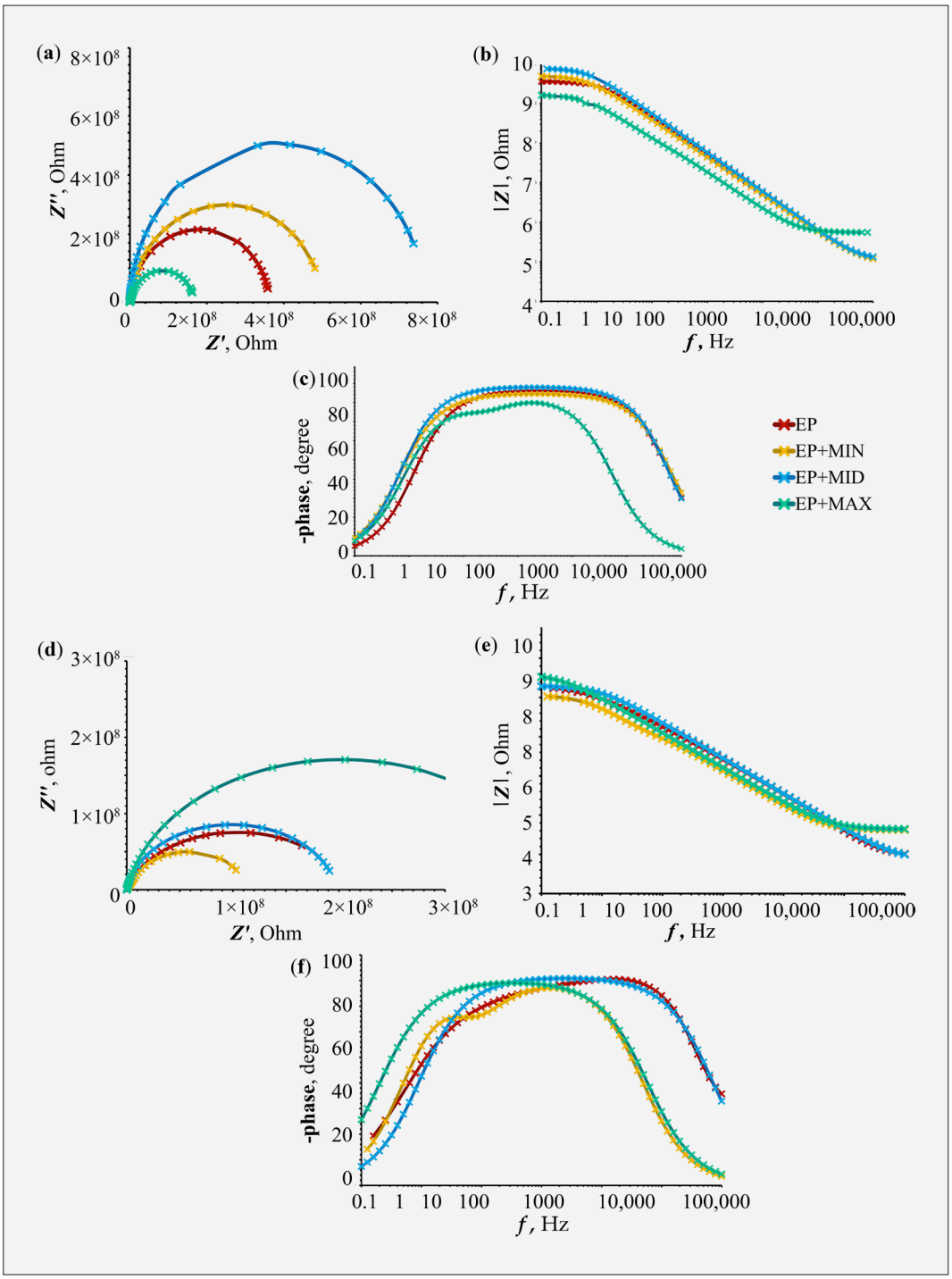

Figure 3. Nyquist and Bode plots of |Z| vs f and phase angle vs. f for epoxy coating, and epoxy coating with minimum, medium, and maximum amount of GO in Al NPs powder immediately (a, b, c) and after 60 days (d, e, f) immersed in 3.5 wt.% NaCl solution.

played in Nyquist and Bode plots (see **Figure 3**). The EIS parameters, including R_e, CPE_{coat}, and R_{coat}, were calculated for the unmodified and modified systems using the equivalent circuit model shown in **Figure 2**. **Table 4** shows the values of the EIS parameters.

The parameter *n* represents the surface conditions, such as surface roughness, metal dissolution and the formation of a porous layer, and varies in the range from 0 to 1 (**Samardžija et al., 2024**). The coating protection efficiency was calculated using the coating resistances and the following equation (**Golabadi et al., 2017**):

$$efficience\ (\%) = \frac{R_{modified\ coat} - R_{EP}}{R_{modified\ coat}} \times 100 \qquad (1)$$

where:

$R_{\text{modified coat}}$ – resistance of EP+MIN, EP+MID or EP+MAX samples (Ω), R_{coat},

R_{EP} – resistance of the epoxy coating (Ω), R_{coat}.

The amount of water absorbed by the coating can be estimated based on its capacity and calculated using the following equation (**Monetta et al., 1993**):

$$\Phi = 100 \times \frac{\log(\frac{CPE_{coat,M}}{CPE_{coat,EP}})}{\log 80} \quad (2)$$

where:

Φ – amount of water taken up by the coating (%),

$\text{CPE}_{\text{coat,M}}$ – capacitance of modify coating EP+MIN, EP+MID, and EP+MAX (F),

$\text{CPE}_{\text{coat, EP}}$ – capacitance of epoxy coating (F).

Immediately after exposure to the corrosive medium, as shown in **Figure 3a**, the electrochemical response of the prepared samples exhibited single constant values. The good adhesion, barrier properties and stability of the unmodified and modified epoxy coating on the grey cast iron substrate can be observed by the appearance of only one capacitive loop in the Nyquist diagram (**Samardžija et al., 2022**, **Sculy et al., 1993**). The sample EP+MAX exhibited the lowest resistance value (R_{coat}) immediately after exposure to the 3.5% NaCl solution, as shown in **Figure 3a**. The corresponding numerical values of the coating resistance are presented in **Table 4**. By adding smaller amount of Al_NPs-GO powder to the epoxy coating, the resistance of the coating increases, resulting in improved durability and an extended service life of the coating. The sample EP+MID exhibited the best corrosion resistance, while the sample EP+MIN showed slightly weaker, but still very good resistance. The disadvantage of the Nyquist diagram is that it does not show the measured value of the impedance in relation to the frequency. Due to this limitation, it is necessary to use the Bode diagram, which enables visualization of the frequency-specific behaviour of the system impedance (**Prakashaiah et al., 2018**). **Figures 3b** and **3c** represent the Bode plot magnitude and Bode phase angle plot for corrosion of unmodified and modified coating samples in 3.5% NaCl solution. Generally, the phase angle varies between 0° which is the case of a perfect resistor, and 90° in the case of a perfect capacitor (**Kalnina et al., 2021**). From the magnitude diagram (see **Figure 3b**), it can be observed that the impedance modulus at low frequencies (log *Z'*) shows the lowest value for the EP+MAX sample, while the EP+MID sample shows the highest corrosion resistance. This resilience is clearly reflected in the numerical values listed in **Table 4**. Similarly, it was observed that the phase maximum at intermediate frequencies for the EP+MAX sample decreased, which can be seen in **Figure 3c**. The EP+MIN sample kept the same phase maximum value as the unmodified EP sample at medium frequencies, while the EP+MID sample showed a slight increase in the phase angle, suggesting that it has a good barrier effect at the beginning of the exposure (**Prakashaiah et al., 2018**). On the other hand, the EP+MAX sample showed the presence of two-time constants, at high frequency 1000 Hz and intermediate frequency of 1 Hz (see **Figure 3c**) which indicates that coating shows some barrier effect (**Tiringer et al., 2018**).

After 60 days of exposure to the corrosive medium, samples EP, EP+MIN, and EP+MID exhibited similar resistance to electrochemical corrosion (see **Figure 3d** and **3e**) whose numerical values are shown in the **Table 4**. This drop in resistance can be attributed to electrolyte penetration through the coating. On the Bode magnitude plot (see **Figure 3e**) for the sample EP+MIN, it can be seen that the electrolyte has penetrated into the microporosity of the organic film, but there is no separation of the coating from the substrate. At a frequency of 1 Hz, we can observe the appearance of a horizontal part of the line at lower frequencies that describes this phenomenon. In general, a decrease in the magnitude of the impedance this region at lower frequency decreases with time until the coating is saturated with electrolyte (**McIntyer and Pham, 1996**). The EP+MAX sample remained intact after 60 days of immersion in a 3.5% NaCl solution, recording a slightly increased impedance value of 405 MΩ, compared to the initial value of 138 MΩ measured at the beginning of exposure (see **Table 4**). Likewise, by analyzing the plot showing the relationship between the angle and the logarithm of the frequency (log *f*), we can see that the transition of the EP+MAX sample moved towards lower frequencies, while the phase angle remained stable at a high level, approximately 80° (see **Figure 3f**). This may be linked to the gradual formation of an oxide passive layer by the Al NPs during immersion, which provides a certain degree of protection (**Tiringer et al., 2018**). (The GO powder in the epoxy coating also served as an effective barrier for defects and microspores, offering excellent protection against the diffusion of oxygen, water, and other corrosive mediums into the coating (**Gaur et al., 2022**). These observations suggest that although it may initially seem that the flakes do not provide immediate protection, their gradual activation contributes to long-term resistance to corrosive effects.

In addition to impedance values for all samples, according to Equation 1, **Table 4** also calculates the effect shown by the modified coatings, both immediately after application and after 60 days of exposure in a 3.5% NaCl solution.

Based on **Table 4**, the coating capacitance (CPE_{coat} value) showed similar values for all samples immediately after being immersed in a 3.5% NaCl solution. The calculated efficiency values show that the EP+MID sample achieves the best improvement in anti-corrosion protection, with an efficiency increase of 58.73%. After 60

Table 4. Data resulted for impedance studies and efficiency after 0 and 60 days of immersion in a 3.5 wt.% NaCl solution

Days	Samples	R_e, Ω	CPE_{coat}, S·sec^n	n_{coat}	R_{coat}, Ω	Efficience, %
0 days	EP	7638	3.86×10^{-10}	0.8383	3.26×10^{8}	-
	EP+MIN	7625	5.10×10^{-10}	0.9168	5.20×10^{8}	37.31
	EP+MID	7646	3.08×10^{-10}	0.8900	7.90×10^{8}	58.73
	EP+MAX	7641	4.54×10^{-10}	0.8307	1.38×10^{8}	-
60 days	EP	7639	1.74×10^{-9}	0.8345	2.13×10^{8}	-
	EP+MIN	7526	2.09×10^{-9}	0.9094	8.71×10^{7}	-
	EP+MID	7633	9.97×10^{-10}	0.8721	2.57×10^{8}	17.12
	EP+MAX	7631	1.98×10^{-10}	0.8908	4.05×10^{8}	47.41

Table 5. Amount of absorbed water (Φ, %) inside the coating after 60 days of exposure in 3.5% NaCl

Sample	EP	EP+MIN	EP+MID	EP+MAX
Φ, %	34.36	32.19	26.81	33.61

days of exposure of the epoxy coating to the corrosive medium, the CPE_{coat} value for all samples increased, indicating that the electrolyte penetrates the coating surfaces. Due to the penetration of the electrolyte, the efficiency of the EP+MID sample, which was the highest at the beginning of exposure, was reduced to 17.12%, while the EP+MAX sample showed the best efficiency values after 60 days, reaching 47.41%. Further analysis of the data presented in **Table 4** reveals that all samples show values for the parameter n between 0.5 and 0.9. These values indicate a pronounced dispersive effect, which is often associated with roughness and surface defects of the coating (**Diaz et al., 2015**).

According to the CPE_{coat} values from **Table 4** and Equation 2, the amount of absorbed water (Φ) in the coating after 60 days of exposure in a 3.5% NaCl solution was calculated. The results of this analysis are presented in **Table 5**.

The amount of absorbed water depends on the thickness of the coating (**Sout et al., 2012**). However, since all samples have the same coating thickness (see **Table 2**), this parameter can be neglected. According to **Table 5**, the unmodified epoxy coating showed the highest level of water absorption, which suggested that its moisture resistance was relatively weaker compared to the modified epoxy formulations. By modifying the epoxy resin, coatings with different levels of water absorption were obtained, where the next in order of water absorption are EP+MAX, EP+MIN, and EP+MID. Cracks and micropores inside the unmodified epoxy coating occur as a result of its exposure to an aggressive corrosive medium, which reduces the resistance and effectiveness of substrate protection. However, the addition of GO to the epoxy coating results in a significant improvement in corrosion protection. Well-dispersed layers of GO are evenly distributed in the structure of the coating, where they fill micropores and cracks, thereby blocking the paths that would otherwise allow the diffusion of corrosive particles (**Jiang et al., 2019**).

3.3. Electrochemical measurement on micro level

To complement the EIS measurements on a macro scale, measurements were conducted on a micro scale at high frequency (100 kHz), where the capacitive behaviour of the coating was observed (see **Figure 4**). Intermittent–contact alternating–current scanning electrochemical microscopy (ic-ac SECM) was applied to obtain a representation of the coating surface in different shades. These shades reflect the electrochemical activity of the surface immediately after exposure to a 3.5% NaCl solution. In this study, the effect of Al_NPs–GO powder in an epoxy coating on corrosion protection was primarily evaluated using ic-ac SECM.

According to **Figures 4a** and **4b**, the unmodified coating shows a uniform distribution of actual impedance resistances (ranging from 107 to 198 kΩ), indicating the homogeneity of the prepared sample. Modified samples with Al NPs–GO powder exhibit slight deviations in homogeneity, which could be due to the uneven distribution of the GO sheet (see **Figures 4d, 4g, 4j**). As the amount of GO within the Al NPs powder increases, the homogeneity of the samples improves (see **Figures 4f, 4i, 4l**). Although the MIN sample shows the most uneven homogeneity, it has the best resistance to electrochemical corrosion. This behaviour may be due to the excessive amount of Al NPs relative to GO. In this sample, not all Al NPs could be incorporated within the GO sheet, leading to free Al NPs that could immediately react with the electrolyte, resulting in the formation of an oxide film on their surface (**Liu et al., 2009**). As the GO content increases, a greater amount of Al NPs is incorporated into the GO structure, which makes the oxidation of Al NPs more difficult.

Capacitance is a key parameter for assessing the penetration of water and corrosive ions into the coating (**Niroumandrad et al., 2016**). At the micro level, the capacitance of the coating (CPE_{coat}) was calculated according to the following expression (**Lazanas et al., 2023**):

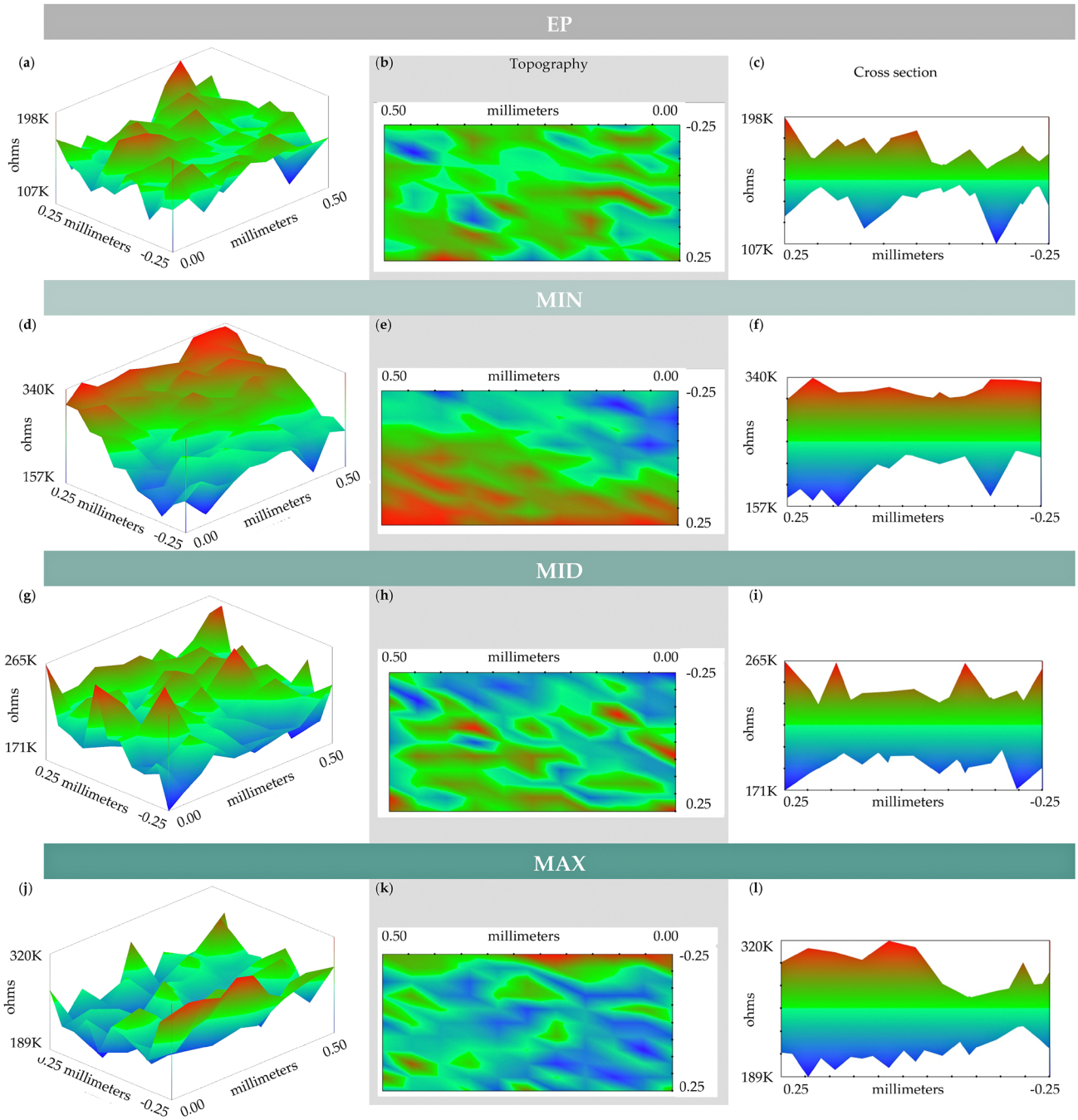

Figure 4. ic-ac SECM distribution of real impedance (Z') at frequency (ω) 100 kHz, topography, and cross-section for: (a, b, c) epoxy coating, (d, e, f) MIN, (g, h, i) MID and (j, k, l) MAX coating sample immediately after being immersed in tap water.

$$\omega = \frac{1}{R_{coat} \times CPE_{coat}} \tag{3}$$

where:

ω – frequency (Hz),

R_{coat} – resistance (Ω),

CPE_{coat} – capacitance of the coating (F).

At high frequencies (100 kHz), the coating resistance (R_{coat}) shows lower values (see **Table 6**) compared to those shown in **Table 4**, where the measurement frequency was 100 mHz. Measurements at high frequencies provide insight into the porosity, i.e. the possibility of electrolyte diffusion through the coating to the surface. According to the R_{coat} values obtained from the impedance maps shown in **Figure 4**, the CPE_{coat} values

Table 6. Data resulted for measured R_{coat} values and calculated CPE_{coat} values for the samples immediately after of immersion in a tap water

Sample	EP	MIN	MID	MAX
R_{coat}, Ω	1.98×10^{5}	3.40×10^{5}	2.65×10^{5}	3.20×10^{5}
CPE_{coat}, F	5.05×10^{-11}	2.94×10^{-11}	3.77×10^{-11}	3.13×10^{-11}

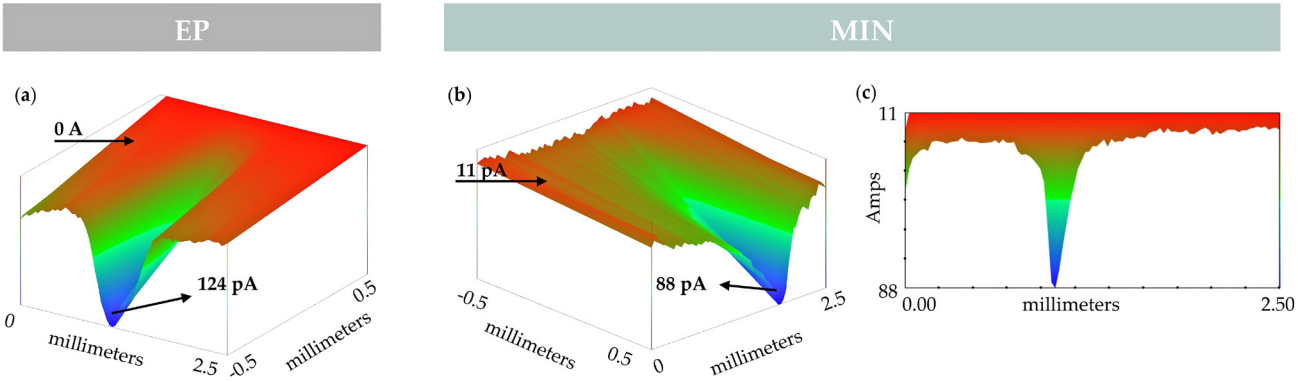

Figure 5. ic-dc SECM distribution of current of scratched samples of: (a) epoxy coating and (b) EP+MIN sample with cross section immediately after immersed in 3.5wt% NaCl solution at the tip potential of +60 V vs Ag/AgCl/KCl reference electrode.

have been calculated using Equation 2. Calculated values are shown in **Table 6**.

According to **Table 6**, the addition of Al NPs–GO powder leads to an increase in the coating resistance (R_{coat}), which reduces the capacitive electrolyte absorption capacity (CPE_{coat}) when the coating is exposed to tap water. As a result, the modified coatings provide more effective corrosion protection compared to the baseline sample.

Electrochemical information, at the tip potential at +0.60 V (vs. Ag/AgCl/ saturated KCl), on the scratches of epoxy coated grey cast iron without and with minimum amount of GO in Al NPs powder immersed in 3.5 wt.% NaCl solution was obtained by SECM images (see **Figure 5**). The colour variation in the SECM images indicates a local anodic area in the scratched sample. The primary anodic reaction during the corrosion of the tested sample in NaCl solution is iron dissolution (**Xavier and Nishimura, 2017**):

$$Fe(s) \rightarrow Fe^{2+}(aq) + 2e^{-} \quad (4)$$

Fe^{2+} ions dissolved in the solution can be detected by setting the tip potential to +0.60 V vs Ag/AgCl, facilitating their oxidation to Fe^{3+} at the tip:

$$Fe^{2+}(aq) \rightarrow Fe^{3+}(aq) + e^{-} \quad (5)$$

E_{TIP} = +0.60 V (vs. Ag/AgCl/saturated KCl).

According to **Figure 5**, both samples exhibit higher current values at the scratch (centre of the sample, indicated by the blue colour). The tip current at the scratch of the epoxy-coated grey cast iron (see **Figure 5a**) shows a higher value than that of the EP+MIN sample (see **Figures 5b** and **5c**). This increase in tip current indicates that the dissolution of Fe^{2+} ions is more pronounced in the epoxy-coated sample. Therefore, we can conclude that the dissolution of Fe^{2+} at the scratch is reduced in the MIN sample compared to the unmodified epoxy coating.

3.4. Evaluation of bacterial biofilm by crystal violet staining

According to the CV staining results, the effects on the biofilm growth inhibition were different (see **Table 6**, **Figure 6**). CV staining had revealed strong biofilm formation in EPO-*S. aureus* (OD 7.12) and moderate biofilm in EPO-*P. aeruginosa* (OD 2.24) compared to control. EPO. MIN- *S. aureus* had moderate biofilm (OD 3.68) and mild biofilm in MIN- *P. aeruginosa* (OD 1.72) compared to control. The MID- *S. aureus* (OD 4.33) and MAX- *S. aureus* (OD 4.76) had strong biofilm. MID- *P. aeruginosa* (OD 1.37) and MAX- *P. aeruginosa* (OD 1.45) had mild biofilm. Furthermore, MIN showed the highest biofilm inhibition activity against *S. aureus* (48%) compared to EPO (see **Table 7**). *S. aureus* biofilm was reduced by 33% by MAX, and 39% by MID compared to the EPO. The biofilm inhibition against *P. aeruginosa* for MAX was 35%, MIN 23% and MID 39% compared to EPO as a control.

Table 7. Categorization of biofilm made by strains *S. aureus* and *P. aeruginosa*,< 1 no biofilm; >1 & <2 mild biofilm; >2 & <4 moderate biofilm; >4 strong biofilm

OD ratio	*S. aureus*	*P. aeruginosa*
EPO	7.12	2.24
MIN	3.68	1.72
MID	4.33	1.37
MAX	4.76	1.45

4. Conclusions

The addition of Al NPs-GO powder inside the epoxy coating results in a change in colour and gloss. Despite these changes in appearance, the key physical properties of the coating, such as hardness, adhesion and thickness, remain unchanged.

The effect of Al NPs–GO powder on epoxy coating on gray cast iron was studied using EIS techniques and ic-ac and ic-dc SECM methods. Classical electrochemical methods, such as EIS, provide insight into the average behaviour of the entire tested surface. According to EIS studies, all modified samples showed an increase in resistance with the addition of Al NPs–GO powder in different periods of exposure in a corrosive medium. The

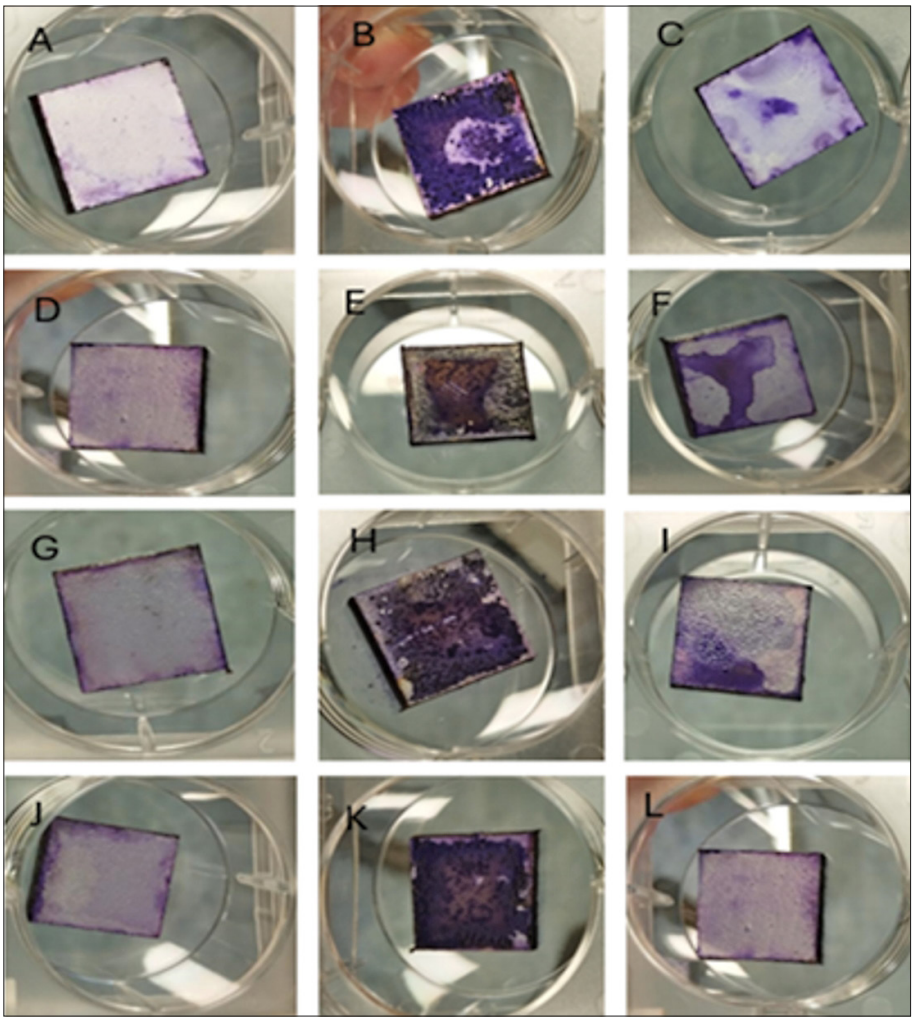

Figure 6. Crystal violet staining of samples, (A) EPO control, (B) EPO-SA, (C) EPO-PAO1, (D) MIN control, (E) MIN-SA, (F) MIN-PAO1, (G) MID control, (H) MID SA, (I) MID PAO1, (J) MAX -control, (K) MAX-SA, (L) MAX-PAO1.

Table 8. Bacterial biofilm percentage (%) inhibition compared to the epoxy (EPO) as a control

Fold change over EPO	MIN	MID	MAX
S. aureus	48%	39%	33%
P. aeruginosa	23%	39%	35%

EP+MAX sample showed stable corrosion protection (about 300 MΩ) for 60 days, while the resistance of other samples decreased. The EP+MAX sample showed the best corrosion protection at the beginning of exposure in a 3.5% NaCl solution. These properties are particularly visible in the fact that the smallest amount of moisture absorption was recorded in that sample, which is 26.81%. These results confirm that the integration of GO into coatings can significantly improve their performance, which is crucial for the development of effective solutions in areas where moisture control is essential. The analysis of the impedance distribution on the surface and the topography of the samples showed that the unmodified sample contains a more homogeneous structure than the modified samples. Measurements made on micro surfaces (of 500 mm) show that there is an increase in impedance values per surface with the addition of Al NPs-GO powder.

Samples EP+MIN and EP+MAX showed the best corrosion resistance. Among all GO samples, MIN showed the highest biofilm inhibition against *S. aureus* and MID sample showed the highest biofilm inhibition against *P. aeruginosa*.

Acknowledgement

This work was supported by the Foundation of the Croatian Academy of Sciences and Arts under the project of "Green synthesis of 2D transition metal carbides: an innovative approach to sustainable production and applications".

5. References

Abdeen, D. H., El Hachach, M., Koc, M., Atieh, M. A. (2019). A review on the corrosion behaviour of nanocoatings on metallic substrates. Materials (Basel). 12,12020210.

Abdullah S.I., Ansari, M.N.M. (2015). Mechanical properties of graphene oxide (GO)/epoxy composites. Housing and Building National Research Center, 11, 151–156.

Abu-Thabit N.Y., Makhlouf, A.S.H. (2015). Recent Advances in Nanocomposite Coatings for Corrosion Protection Applications. Elsevier Ltd., 2015.

Aghili, M., Yazdi, M. K., Ranjbar, Z., Jafari, S. H. (2021). Anticorrosion performance of electro-deposited epoxy/ amine functionalized graphene oxide nanocomposite coatings. Corrosion Science, 179, 109143.

Chauhan D. S., Quraishi M. A., Ansari K. R., Saleh T. A. (2020). Graphene and graphene oxide as new class of materials for corrosion control and protection: Present status and future scenario. Progress in Organic Coatings 147, 105741.

Chee, W.K., Lim, H.N., Huang, N.M., Harrison I. (2015). Nanocomposites of graphene polymers a review, RSC Advances, 5, 68014–68051.

Deyab, M.A., De Riccardis, A., Mele, G. (2016). Novel epoxy/ metal phthalocyanines nanocomposite coatings for corrosion protection of carbon steel. Journal of Molecular Liquids, 220, 513–517.

Diaz, E.F., Cuevas-Arteaga, C., Flores-García, N., Mejía Sintillo, S., Sotelo-Mazón, O. (2015). Corrosion Performance of AISI-309 Exposed to Molten Salts V2O5-Na2SO4 at 700°C Applying EIS and Rp Electrochemical Techniques. Journal of Spectroscopy, 2015, 826759.

Duan Z. (2019). Application of graphene in metal corrosion protection. IOP Conference Series. Material Science and Engineering, 496, 012020.

Gaur, M.S., Raghav, R.K., Sagar, R., Tiwari, R.K. (2022). Investigation of anticorrosion properties of epoxy GO nanocomposites spin coatedAluminum Alloy 7075. Polymers and Polymers Composites, 30, 1–10.

Golabadi, M., Aliofkhazraei, M., Toorani, M., Sabour Rouhaghdam, A. (2017). Corrosion and cathodic disbondment resistance of epoxy coating on zinc phosphate conversion coating containing Ni^{2+} and Co^{2+}. Journal of Industrial and Engineering Chemistry, 47, 154–168.

ISO 868 (2003). Plastic and ebonite—Determination of indentation hardness by means of a durometer (Shore hardness). International Organization for Standardization: Geneva, Switzerland, https://www.iso.org/standard/34804.html

ISO 2813 (2000). Paints and varnishe –Determination of specular gloss of non–metallic paint films at 20°, 60°, and 85°. International Organization for Standardization: Geneva, Switzerland, https://www.iso.org/standard/56807.html

Jiang, F.; Zhao, W.; Wua, Y.; Dong, J.; Zhou K.; Lu, G.; Pu, J. (2019). Anti-corrosion behaviors of epoxy composite coatings enhanced via graphene oxide with different aspect ratios. Progress in organic Coating, 127, 70–79.

Kabeb, S. M., Hassan, A., Mohamad, Z., Sharer, Z., Mokhtar, M., Ahmad, F. (2018). Exploring the effects of nanofillers of epoxy nanocomposite coating for sustainable corrosion protection. Chemical Engineering Transactions, 72, 121–126.

Karthikaiselvi R., Subhashini, S. (2014). Study of adsorption properties and inhibition of mild steel corrosion in hydrochloric acid media by water soluble composite poly (vinyl alcohol-o-methoxy aniline). Journal of the Association of Arab Universities for Basic and Applied Sciences, 16, 74–82.

Kim, H., Abdala, A.A., Macosko C.W. (2010). Graphene/Polymer nanocomposites. Macromolecules, 43, 6515–6530.

Kumar, S.S.A., Bashir, S., Ramesh, K., Ramesh, S. (2021). New perspectives on Graphene/Graphene oxide based polymer nanocomposites for corrosion applications: The relevance of the Graphene/Polymer barrier coatings. Progress in Organic Coatings, 154, 106215.

Lazanas, A.C., Prodromidis, M.I. (2023). Electrochemical Impedance Spectroscopy – A Tutorial. ACS Measurement Science Au Journal, 3, 162–193.

Liu, X., Xiong, J., Lv, Y., Zuo, Y. (2009). Study on corrosion electrochemical behavior of several different coating systems by EIS. Progress in Organic Coating, 64, 497–503.

Ljubek, G., Čapeta, D., Šrut Rakić., Kraljić Roković, M. (2021). Energetically efficient and electrochemically tuneable exfoliation of graphite: process monitoring and product characterization. Journal of materials science, 56, 10859-10875.

McIntyre, J.M.; Pham, H.Q. (1996). Electrochemical impedance spectroscopy; a tool for organic cating optimization. Pregress in Organic Coatings 27, 201–207.

Mohammadi, S., Afshar Taromi, F., Shariatpanahi, H., Neshati, J., Hemmati, M. (2014). Electrochemical and anticorrosion behavior of functionalized graphite nanoplatelets epoxy coating. Journal of Industrial and Engineering Chemistry, 20, 4124–4139.

Monetta, T., Belluci, F., Nicodemo, L., Nicolais, L. (1993). Protective properties of epoxy-based organic coatings on mild steel. Progress in Organic Coating 21 353–369.

Muresan, L. M. (2023) Nanocomposite Coatings for Anti-Corrosion Properties of Metallic Substrates. Materials (Basel)., 16.

Niroumandrad, S., Rostami, M., Ramezanzadeh, B. (2016). Effects of combined surface treatments of aluminium nanoparticle on its corrosion resistance before and after inclusion into an epoxy coating. Progress in Organic Coating, 101, 486–501.

Nguyen-tri, P., Nguyen, T.A., Carriere, P., Xuan C.N. (2018). Nanocomposite Coatings: Preparation, Characterization, Properties, and Applications. International Journal of Corrosion, 2018, 4749501.

Prakashaiah, B.G.; Vinaya Kumara, B., Anup Pandith A., Nityananda Shetty, A., Amitha Rani B.E. (2018). Corrosion inhibition of 2024-T3 aluminum alloy in 3.5% NaCl by thiosemicarbazone derivatives. Corrosion Science, 15, 326-338.

Rezvani Moghaddam, A., Ranjbar, Z., Sundararaj, U., Jannesari, A. (2019). A novel electrically conductive water borne epoxy nanocomposite coating based on graphene: facile method and high efficient graphene dispersion. Progress in Organic Coating, 136, 105223.

Sadasivuni, K. K., Ponnamma D., Kim, J., Thomas, S. (2015): Graphene-based polymer nanocomposites in electronics,

Publisher: Springer: Switzerland, Springer Series on Polymer and Composite Materials, ISBN 978-3-319-13875-6

Samardžija, M., Alar, V., Špada, V., Stojanović, I. (2022). Corrosion Behaviour of an Epoxy Resin Reinforced with Aluminium Nanoparticles. Coatings, 12, 12101500.

Samardžija, M., Stojanović, I., Kurtela, M., Alar, V. (2024). Influence of aluminum nanoparticles in epoxy resin and epoxy coating for anticorrosion and antibacterial protection in pipeline industry. Journal of Applied Polymer Science, 141, 1–14.

Samardžija, M., Alar, V., Aljinović, F., Kapor, F. (2022). Influence of phosphate layer on adhesion properities between a steel surface and an organic coating. Rudarsko-geološko-naftni zbornik, 37, 11–17.

Samyn, P.; Erps, J.V., Thienpont, H. (2015). Specular gloss versus surface topography for oil-filled nanoparticle coatings on paper. Color Research & Application, 41, 596–610.

Sculy, J.R., Silverman, D.C., Kendig, M.W. (1993). Electrochemical Impedance: Analysis and Interpretation; ASTM Publication: Philadelphia, PA, USA.

Sout, R.M.; Moreno, C.; Hernández, S.; Rodríguez, J.J.S.; González-Guzmán, J.; Gonzalez, S. (2012). Characterization of Water Uptake by Organic Coatings Used for the Corrosion Protection of Steel as Determined from Capacitance Measurements. International Journal of Electrochemical Science, 7, 7390–7403.

Tiringer, U., Durán, A., Castro, Y., Milošev, I. (2018). Self-Healing Effect of Hybrid Sol-Gel Coatings Based on GPTMS, TEOS, SiO_2 Nanoparticles and $Ce(NO_3)_3$ Applied on Aluminum Alloy 7075-T6. Journal of Electrochemical Society, 165, C213–C225.

Xavier, J.R., Nishimura, T. (2017). Evaluation of the corrosion protection performance of epoxy coatings containing Mg nanoparticle on carbon steel in 0.1 M NaCl solution by SECM and EIS techniques. Journal of Coatings Technology and Research, 14, 395–406.

Wu, Y., Yu, J., Zhao, W., Wang, C., Wu, B., Lu, G. (2019). Investigating the anti-corrosion behaviors of the waterborne epoxy composite coatings with barrier and inhibition roles on mild steel. Progress in organic caotings, 199, 8–18.

SAŽETAK

Istraživanje otpornosti na koroziju epoksidnih prevlaka pojačanih grafenovim oksidom i aluminijevim nanočesticama

Grafenov oksid (GO) dvodimenzionalni je ugljikov nanomaterijal poznat po iznimnnoj mehaničkoj čvrstoći i prilagodljivoj, funkcionalnoj površini, što ga čini obećavajućim materijalom za zaštitne barijere protiv štetnih vanjskih utjecaja. U tu svrhu koristi se kao punilo u epoksidnim premazima kako bi se povećao vijugavi put difuzije korozivnoga medija unutar prevlake. Pored toga, unošenje aluminijskih nanočestica (Al NP) na površinu GO može poboljšati disperziju GO listova, smanjiti njihovu agregaciju i održati pasivni oksidacijski film koji nastaje razgradnjom Al NP. U ovoj studiji pripremljeni su epoksidni premazi koji sadržavaju prah Al NP–GO s različitim težinskim udjelima GO materijala. Procijenjena su fizička, antikorozivna i antibakterijska svojstva nemodificiranih i modificiranih prevlaka. Na makroskopskoj elektrokemijskoj mikrorazini uzorak EP+MAX pokazuje stabilnu zaštitu od korozije tijekom 60 dana, dok je otpor ostalih uzoraka smanjen. Mjerenja obavljena na mikropovršinama (od 500 μm) pokazuju da dolazi do povećanja vrijednosti impedancije po površini s dodatkom praha Al NPs-GO. Najbolju otpornost na koroziju pokazali su uzorci EP+MIN i EP+MAX. Također, primjenom ic-dc mikroskopske SECM metode utvrđeno je da je otapanje Fe^{2+} na ogrebotini smanjeno kod modificiranih uzoraka. Dodatno, pokazalo se da epoksidna prevlaka stječe nova antibakterijska svojstva, čime dobija dvostruku funkcionalnost.

Ključne riječi:
korozijska zaštita, antibakterijsko djelovanje, epoksidna prevlaka, aluminijeve nanočestice, grafenov oksid

Author's contribution

Marin Kurtela (PhD at the Faculty of Mechanical Engineering and Naval Architecture) provided sample collection**,** data interpretation, technical suggestions, conceptualization, supervised the experiments, wrote the introduction part of article, project administration. **Marina Samardžija** (PhD student at the Faculty of Chemical Engineering and Technology, University of Zagreb) formed the object and the subject of the research, conceptualization, proposed the idea, developed the idea of the work and the methodology for achieving results, analysis of the research, wrote the experimental and discussion part of the article. **Maro Bujak** (PhD) formed an idea for testing the antibacterial properties of the coating, interpreted the results for the antibacterial effect of the coating, data curation, writing-review and editing. **Ivan Stojanović** (PhD, Associate Professor at Faculty of Mechanical Engineering and Naval Architecture) supervision visualization, writing-review and editing. **Krunoslav Bojanić** (PhD) supervision. **Ljubek Gabrijela** (PhD at the Faculty of Mining Geology and Petroleum Engineering) proposed the idea, and contributed with supervision, writing-review and editing.
All authors have read and agreed to the published version of the manuscript.